J. Phys. C: Solid St. Phys., 1971. Vol. 4. Printed in Great Britain

# Excitations in $KCoF_3$ II. Theoretical

W. J. L. BUYERS,† T. M. HOLDEN,† E. C. SVENSSON,† R. A. COWLEY†§ and M. T. HUTCHINGS‡¶

†Atomic Energy of Canada Limited, Chalk River, Ontario, Canada

‡Clarendon Laboratory, Oxford University, and Brookhaven National Laboratory, Upton, New York 11973, USA

*MS. received 24th November 1970*

**Abstract.** The theory of the low lying magnetic excitations of $KCoF_3$ is developed and the parameters describing the magnetic interactions are obtained by comparison with the experimental results of the previous paper. The branch of the elementary excitation spectrum of lowest frequency is well described by a phenomenological model with an effective spin $s' = \frac{1}{2}$. The exchange interaction has the Heisenberg form, and the pseudo-dipolar form of anisotropic exchange proposed recently for $KCoF_3$ is shown to be less than 8% of the isotropic exchange. A model which takes the orbital angular momentum of the $Co^{2+}$ ion into account is developed by relating the elementary excitations to the quasiboson excitations between the ground state and all eleven excited states of the $^4T_1$ orbital level. This model fits the experimental results for the two branches of lowest frequency extremely well. The interaction between real spins is found to be of the Heisenberg form and the spin–orbit coupling constant is found to be 82% of the free ion value. Calculations of the relative intensity of neutron scattering as a function of wavevector transfer for the modes belonging to the two lowest branches of magnetic excitations give good agreement with experiment. The origin of the magnon–phonon interaction is discussed mainly in terms of the crystal field acting on the $Co^{2+}$ ions caused by the motion of the surrounding fluorine ions in the $\Gamma_{25}$ phonon modes.

## 1. Introduction

In the preceding paper (Holden *et al.* 1971, to be referred to as I) neutron inelastic scattering measurements of the magnons and phonons in the antiferromagnet $KCoF_3$ were described. In this paper the theory of the magnetic excitations at low temperatures in $KCoF_3$ is discussed and from the measurements the parameters describing the exchange interactions and anisotropy constants are deduced.

The magnetic properties of $KCoF_3$ are of particular interest because the orbital angular momentum of the $Co^{2+}$ ion is not quenched by the octahedrally coordinated crystal field. This gives rise to the possibility of anisotropic magnetic interactions between the ions and to the presence of excited states whose energies may be sufficiently close to the ground state to affect its properties considerably.

In § 2 the single ion properties of the $Co^{2+}$ ion and the nature of the exchange interactions between ions are reviewed. Most of the measurements reported in I were of the lowest branch of the magnetic excitations, and these excitations may be described by an effective spin $\frac{1}{2}$ model as described in § 3. A more complete theory, involving the mixing between the different levels, is described in § 4, and the exchange constant, spin–orbit parameter and distortion energy are derived from fitting this many level model to the observed frequencies of magnetic excitations. The one-magnon neutron scattering cross section is

§ Now at University of Edinburgh, Scotland.

¶ Now at AERE, Harwell, Didcot, Berkshire.

calculated in § 5 from the many level model and found to be in good agreement with experiment. One of the more interesting features of the experimental results (I) was the observation of a strong magnon–phonon interaction. The nature of this interaction is discussed in § 6.

## 2. Single ion properties

The Hamiltonian for the lowest energy states in $KCoF_3$ may be written

$$\mathscr{H} = \mathscr{H}_{\text{cubic}} + \mathscr{H}_{\text{tetrag}} + \mathscr{H}_{\text{so}} + \mathscr{H}_{\text{ex}}$$

where the first two terms describe the tetragonally distorted cubic crystal field, the third term the spin–orbit coupling, and the fourth term the interactions, exchange and dipolar, between the ions. $\mathscr{H}_{\text{ex}}$ may in principle include both isotropic and anisotropic exchange terms. It is convenient to split $\mathscr{H}$ into two parts

$$\mathscr{H} = \mathscr{H}^{(1)} + \mathscr{H}^{(2)}. \tag{1}$$

$\mathscr{H}^{(1)}$ contains the single ion terms

$$\mathscr{H}^{(1)} = \mathscr{H}_{\text{cubic}} + \mathscr{H}_{\text{tetrag}} + \mathscr{H}_{\text{so}} + \mathscr{H}_{\text{mf}}$$

where the last term describes the molecular field part of the exchange energy and anisotropy energy, and

$$\mathscr{H}^{(2)} = \mathscr{H}_{\text{ex}} - \mathscr{H}_{\text{mf}}.$$

In this section the Hamiltonian $\mathscr{H}^{(1)}$ is solved to give a set of local excitations whose residual interactions $\mathscr{H}^{(2)}$ give rise to the magnons as discussed in §§ 3 and 4.

### 2.1. *The crystal field and spin–orbit interaction*

The theory of the energy levels and wavefunctions of a $Co^{2+}$ ion in an octahedrally coordinated cubic environment with small tetragonal distortions was first discussed by Abragam and Pryce (1951) and by Thornley *et al.* (1965) in more detail. The intra-ion

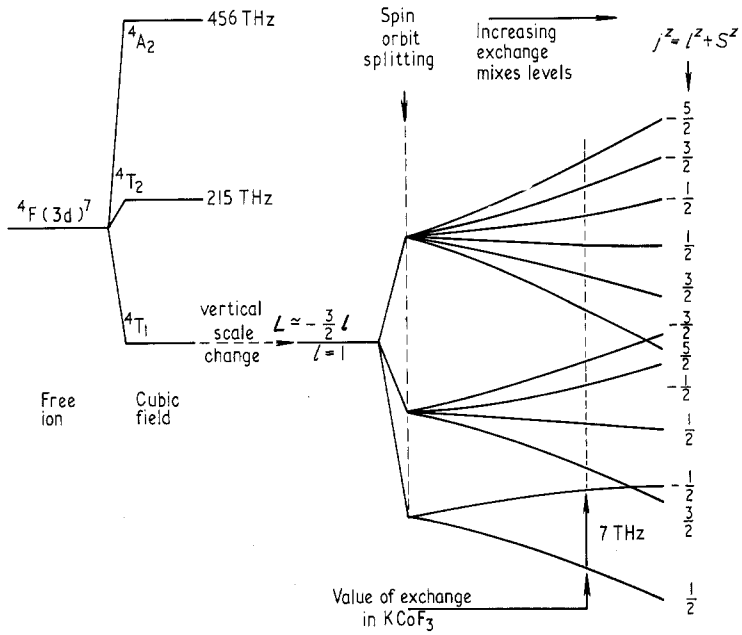


Figure 1. Energy levels of $Co^{2+}$ ions in $KCoF_3$ as a function of the molecular field energy.

electrostatic interaction is treated first, then the cubic crystal field with possible distortions, and finally the spin–orbit coupling. A schematic diagram of the splitting of the levels is shown in figure 1.

The ground term of the $(3d)^7$ configuration of the free $Co^{2+}$ ion is $^4F$. The next term level $^4P$ lies about 14000 $cm^{-1}$ above this and the crystal field causes a small admixture with the ground term. An octahedral field splits the $^4F$ term into a singlet and two triplet states as shown in figure 1. The ground $^4T_1$ orbital triplet has the same symmetry as a manifold of p states and the matrix elements of the true angular momentum operator $\boldsymbol{L}$ may be conveniently represented by those of $-\alpha\boldsymbol{l}$, where $\boldsymbol{l}$ is an effective orbital operator acting within a manifold of states with $l = 1$. If admixture of the $^4P$ term is neglected, $\alpha = \frac{3}{2}$. The effect of inclusion of the $^4P$ levels is to reduce $\alpha$, and Thornley *et al.* (1965) find a value of 1·421 for $Co^{2+}$ ions in $KMgF_3$. To allow for covalency, the operator $\boldsymbol{l}$ may be reduced by a further factor $k_{orb}$, the orbital reduction factor (Stevens 1953), which Thornley *et al.* estimate from experiment to be 0·93 (±0·03). A small tetragonal distortion will remove the degeneracy of the orbital triplet in a manner described by the effective Hamiltonian

$$\mathscr{H}_{tetrag} = c(l_z^2 - \tfrac{2}{3})$$

where $c$ includes the reduction factor $k_{orb}^2$, but this distortion is thought to be very small in the low temperature phase of $KCoF_3$ (Okazaki and Suemune 1961).

Spin–orbit coupling gives rise to an effective Hamiltonian, $\mathscr{H}_{so} = -\lambda'\alpha\boldsymbol{l}.\boldsymbol{S}$, acting within the $^4T_1$ states. If there is no distortion of the cubic field, $\boldsymbol{l}$ and $\boldsymbol{S}$ are coupled as in rare earth ions to give multiplets characterized by a given value of $\boldsymbol{j} = \boldsymbol{l} + \boldsymbol{S}$. In the free $Co^{2+}$ ion the value of the spin–orbit coupling constant $\lambda$ is $-178$ $cm^{-1}$, but this will be reduced in the crystal by the covalency to a value $\lambda'$ which may best be estimated from experiments involving only the $^4T_1$ states. Thornley *et al.* estimate from the susceptibility data of Hirakawa *et al.* (1960) that $\lambda' = -160 \pm 10\,cm^{-1}$ for $KCoF_3$. In a weak magnetic field the multiplets will be split by the perturbation Hamiltonian

$$\begin{aligned}\mathscr{H}_m &= \mu_B(\boldsymbol{L} + 2\boldsymbol{S}).\boldsymbol{H}\\ &= \mu_B(-\alpha\boldsymbol{l} + 2\boldsymbol{S}).\boldsymbol{H}\\ &= g_j\mu_B\boldsymbol{H}.\boldsymbol{j}.\end{aligned}$$

Here $\mu_B$ is the Bohr magneton, and $g_j$ is an effective Landé $g$ factor for the multiplet which is readily shown to be given by

$$g_j = \frac{(2-\alpha)j(j+1) - (2+\alpha)l(l+1) + (2+\alpha)S(S+1)}{2j(j+1)}.$$

For the lowest doublet $g_j = \frac{1}{3}(10 + 2\alpha)$, $= 13/3$ if $\alpha = \frac{3}{2}$. If we represent the interaction with a magnetic field by an effective spin Hamiltonian, $\mathscr{H}_m = \mu_B\boldsymbol{H}.\mathbf{g}.\boldsymbol{S}'$, then $\mathbf{g}$ is a diagonal matrix of magnitude $g_j$ and the effective spin $S' = j = \frac{1}{2}$. Furthermore, the matrix elements of the true spin within the ground doublet states may be found from the relation

$$\boldsymbol{S} = \frac{g_j + \alpha}{2 + \alpha}\boldsymbol{S}' = \tfrac{5}{3}\boldsymbol{S}' \qquad \text{when } \alpha = \tfrac{3}{2}. \tag{2}$$

The effect of a small tetragonal distortion will be to cause the matrix $\mathbf{g}$ to become axially anisotropic about the unique axis. It should be noted that in the presence of exchange interactions between the ions, the effective field in the antiferromagnetic state is no longer weak so that the above relations are modified by the mixing with higher levels as will be seen in § 2.3.

### 2.2. *The exchange interaction*

The exchange interaction between ions with large orbital contributions to their moments has been discussed by several authors (Van Vleck 1962, Levy 1964, 1966, Elliott and Thorpe

1968, Birgeneau *et al.* 1969). The exchange interaction between the individual electrons of each of the ions depends on their orbital wavefunctions. When these interactions are summed and projected on to the manifold of $^4T_1$ states it is found that the exchange interaction $J$ (see equation (4) below) must be replaced by products of orbital operators acting on each ion, which transform like spherical harmonics. When projected on to a $j$ multiplet the resulting interaction may contain terms of high degree in the operators $j_x$, $j_y$ and $j_z$. In each case the pair interaction may show a different anisotropy from that expected on simple grounds, though it must of course be consistent with the overall symmetry.

Elliott and Thorpe (1968) and Copland and Levy (1969) discuss the form of exchange in $KCoF_3$ by considering only the lowest doublet ($S' = \frac{1}{2}$) and a cubic crystal structure. They show that the form of exchange between two $Co^{2+}$ ions may be anisotropic along the bond joining the pairs of atoms; that is, the interaction $J'$ is different when the spins are parallel to the bond, $J'_{\parallel}$, or perpendicular to the bond $J'_{\perp}$. For example, for the pairs of atoms separated by a distance $(a, 0, 0)$ the interaction is

$$\mathscr{H}_{ex}^{12} = 2J'_{\parallel}(12)S'_x(1)S'_x(2) + 2J'_{\perp}(12)\{S'_y(1)S'_y(2) + S'_z(1)S'_z(2)\}. \tag{3}$$

Elliott and Thorpe (private communication) estimate that the anisotropy

$$\left|2\left(\frac{J_{\parallel} - J_{\perp}}{J_{\parallel} + J_{\perp}}\right)\right|$$

may be as large as 0·2 while Copland and Levy estimate it to be about 0·3. This form of directional exchange may be tested by our experimental results.

In most of our calculations the exchange interaction between real spins is assumed to be

$$\mathscr{H}_{ex}^{12} = 2J(12)\boldsymbol{S}(1) \cdot \boldsymbol{S}(2). \tag{4}$$

This form of interaction may be projected onto the ground state to give the effective exchange constant. If we ignore the mixing of the $j$ multiplets then from equation (2) the interaction between the effective spins is

$$\mathscr{H}_{ex}^{12} = 2J'(12)\boldsymbol{S}'(1) \cdot \boldsymbol{S}'(2) \tag{5}$$

where $J'(12) = \{(g_j + \alpha)/(2 + \alpha)\}^2 J(12) = (25/9)J(12)$ when $\alpha = \frac{3}{2}$. On this simplified model, when the ground state is perturbed by a tetragonal distortion, the effective spin Hamiltonian may have the axial form

$$\mathscr{H}_{ex}^{12} = 2J'_z(12)S'_z(1)S'_z(2) + 2J'_x(12)\{S'_x(1)S'_x(2) + S'_y(1)S'_y(2)\} \tag{6}$$

where $z$ lies along the distortion axis and the anisotropy is the same as in $\tilde{\mathbf{g}} \cdot \mathbf{g}$.

### 2.3. *The molecular field approximation to the total Hamiltonian*

The effect of the exchange interactions between the $Co^{2+}$ ions is now discussed using the molecular field approximation. This provides a first order solution of the energy levels and states of the system on which a complete spin-wave theory is based. It also serves to estimate the magnitude of the effect of the excited states on the magnetic properties of the ground state due to admixtures by the exchange field.

The molecular field solution is obtained from the single ion Hamiltonian of equation (1). The molecular field part of the Hamiltonian, $\mathscr{H}_{mf}$, is obtained from the total exchange energy

$$\mathscr{H}_{ex} = \sum_{jk} \sum_{j'k'} J \begin{pmatrix} j & j' \\ k & k' \end{pmatrix} \boldsymbol{S}(jk) \cdot \boldsymbol{S}(j'k') \tag{7}$$

where the sums run over the cells $j$ and ions within a cell $k$ ($k = 1, 2$ for the two sublattice antiferromagnet) of the magnetic lattice. The molecular field Hamiltonian is

$$\mathscr{H}_{mf} = \sum_{jk} (-1)^k (H_a + H_z) S_z(jk) \tag{8}$$

with the molecular field

$$H_z = 2\sum_r Z_r J_r \langle S_z \rangle \tag{9}$$

where $J_r$, $Z_r$ are the exchange constant and number of the $r$th neighbours and $\langle S_z \rangle$ is the sublattice magnetization. The molecular field solution of the present section is thus based on the single ion Hamiltonian. which within the $^4T_1$ state is

$$\mathscr{H}^{(1)} = \sum_{jk} h_k(j)$$

$$h_k = \Lambda \boldsymbol{l}.\boldsymbol{S} + cl_z^2 + (-1)^k(H_a + H_z)S_z \tag{10}$$

where $\Lambda = -\alpha\lambda'$ is the apparent spin–orbit parameter. We represent the anisotropy by the effective field $H_a$. Since dipolar anisotropy is absent in a cubic material and since crystal field anistropy does not affect the ground doublet in the absence of mixing, the anisotropy field must result mainly from anisotropic exchange and is therefore expected to be small.

**Table 1. Wavefunctions of the lowest single ion states of the $Co^{2+}$ ion in an octahedral field**

| $p$ | | $\nu_p$ | Contributions from states $\lvert l_z, s_z\rangle$ | | |
|---|---|---|---|---|---|
| | | | $\lvert 1, -\frac{1}{2}\rangle$ | $\lvert 0, \frac{1}{2}\rangle$ | $\lvert -1, \frac{3}{2}\rangle$ |
| 0 | NM | 0 | 0·408 | −0·577 | 0·707 |
| | M | 0 | 0·215 | −0·470 | 0·856 |
| | | | $\lvert -1, \frac{1}{2}\rangle$ | $\lvert 0, -\frac{1}{2}\rangle$ | $\lvert 1, -\frac{3}{2}\rangle$ |
| 1 | NM | 0 | 0·408 | −0·577 | 0·707 |
| | M | 7·06 | 0·671 | −0·600 | 0·437 |
| | | | $\lvert 1, \frac{1}{2}\rangle$ | $\lvert 0, \frac{3}{2}\rangle$ | |
| 2 | NM | 9·49 | −0·632 | 0·775 | |
| | M | 8·92 | −0·528 | 0·849 | |
| | | | $\lvert 1, -\frac{1}{2}\rangle$ | $\lvert 0, \frac{1}{2}\rangle$ | $\lvert -1, \frac{3}{2}\rangle$ |
| 3 | NM | 9·49 | −0·730 | 0·258 | 0·632 |
| | M | 12·96 | −0·712 | 0·524 | 0·466 |
| | | | $\lvert -1, \frac{1}{2}\rangle$ | $\lvert 0, -\frac{1}{2}\rangle$ | $\lvert 1, -\frac{3}{2}\rangle$ |
| 4 | NM | 9·49 | −0·730 | 0·258 | 0·632 |
| | M | 16·64 | −0·608 | −0·108 | 0·787 |
| | | | $\lvert -1, -\frac{1}{2}\rangle$ | $\lvert 0, -\frac{3}{2}\rangle$ | |
| 5 | NM | 9·49 | −0·632 | 0·775 | |
| | M | 18·75 | −0·737 | 0·676 | |

The frequency (energy) of each state is given in units of THz and the fraction of each $\lvert l_z S_z\rangle$ component of the state is given as a normalized eigenvector. For each state the wavefunction is given for the case of zero molecular field (NM), previously quoted by Thornley *et al.* (1965), and for the molecular field appropriate to $KCoF_3$ in its classical ground state (M) ($J$ = 0·308 THz), as given by model A of table 5.

The molecular field energies $h\nu_p = E_p - E_0$ and wavefunctions $\lvert p\rangle$ ($p$ = 0–11) have been obtained by diagonalizing the 12 × 12 single-ion Hamiltonian equation (10) as a function of the molecular field $H_a + H_z$. In table 1 the results for the six states of lowest energy are shown both for the case of zero molecular field and for the molecular field found to be appropriated for $KCoF_3$ at low temperature. Table 2 gives the relevant matrix elements of $\boldsymbol{l}$ and $\boldsymbol{S}$. The energies of the states as a function of molecular field strength shown in figure 1 indicate that at the field strength appropriate to $KCoF_3$ there is appreciable mixing of the levels. The nonsymmetrical splitting and curvature of the lowest pair of

**Table 2. Matrix elements of $S$ and $l$ within the lowest five states of the $Co^{2+}$ ion for the wavefunctions of table 1**

| $p$ | $\nu_p$ | $\langle p\|S_+\|0\rangle$ | $\langle p\|S_-\|0\rangle$ | $\langle p\|S_z\|0\rangle$ | $\langle p\|S_z\|p\rangle$ | $\langle p\|l_+\|0\rangle$ | $\langle p\|l_-\|0\rangle$ | $\langle p\|l_z\|0\rangle$ | $\langle p\|l_z\|p\rangle$ |
|---|---|---|---|---|---|---|---|---|---|
| *States in zero molecular field (NM)* | | | | | | | | | |
| 0 | 0 | 0 | 0 | 0·833 | 0·833 | 0 | 0 | −0·333 | −0·333 |
| 1 | 0 | 0 | 1·667 | 0 | −0·833 | 0 | −0·667 | 0 | +0·333 |
| 2 | 9·49 | −1·291 | 0 | 0 | 1·100 | 1·291 | 0 | 0 | 0·400 |
| 3 | 9·49 | 0 | 0 | 0·745 | 0·367 | 0 | 0 | −0·745 | 0·133 |
| 4 | 9·49 | 0 | −0·745 | 0 | −0·367 | 0 | 0·745 | 0 | −0·133 |
| 5 | 9·49 | 0 | 0 | 0 | −1·100 | 0 | 0 | 0 | −0·400 |
| *States in molecular field of $KCoF_3$(M)* | | | | | | | | | |
| 0 | 0 | 0 | 0 | 1·187 | 1·187 | 0 | 0 | −0·687 | −0·687 |
| 1 | 7·06 | 0 | 1·721 | 0 | −0·241 | 0 | −0·628 | 0 | −0·259 |
| 2 | 8·92 | −0·918 | 0 | 0 | 1·221 | 1·379 | 0 | 0 | 0·279 |
| 3 | 12·96 | 0 | 0 | 0·552 | 0·210 | 0 | 0 | −0·552 | 0·210 |
| 4 | 16·64 | 0 | −0·508 | 0 | −0·749 | 0 | 0·371 | 0 | 0·249 |
| 5 | 18·75 | 0 | 0 | 0 | −0·957 | 0 | 0 | 0 | −0·543 |

The upper half of the table has been calculated from the unmixed states and the lower half from the exchange mixed states. The latter were used in the calculation of the properties of the local magnetic mode of the $Co^{2+}$ ion in $KMnF_3$ (Svensson *et al.* 1969).

levels as a function of field, and the nonzero average value of $l_z$ and $S_z$ in these states (table 2) result from the mixing.

## 3. The spin $\frac{1}{2}$ model

In this section the simple effective spin one half model is used to describe the lowest frequency branch of the magnetic excitations in $KCoF_3$.

### 3.1. *The effective spin Hamiltonian*

The effective spin Hamiltonian for the exchange and anisotropy energies (equations (7) and (10)) within the two states of lowest energy is

$$\mathscr{H}_{\text{eff}} = \sum_{jj'} \sum_{kk'} J' \begin{pmatrix} j & j' \\ k & k' \end{pmatrix} \boldsymbol{S}'(jk) . \boldsymbol{S}'(j'k') + \sum_{jk} (-1)^k H'_a S'_z(jk). \tag{11}$$

The frequencies of the spin waves are then given by

$$h\nu(\boldsymbol{q}) = (\{H'_a + 2S'\{J'(12, 0) - J'(11, 0) + J'(11, \boldsymbol{q})\}\}^2 - \{2S'J'(12, \boldsymbol{q})\}^2)^{\frac{1}{2}} \tag{12}$$

where

$$J'(kk', \boldsymbol{q}) = \sum_{j'} J' \begin{pmatrix} j & j' \\ k & k' \end{pmatrix} \exp [i\boldsymbol{q} . \{\boldsymbol{R}(jk) - \boldsymbol{R}(j'k')\}]. \tag{13}$$

The parameters $J' \begin{pmatrix} j & j' \\ k & k' \end{pmatrix}$ and $H'_a$ may be obtained by fitting the observed magnon frequencies (I). They may be related to the parameters of the exchange and anisotropy of the real spin system (equations (7) and (10)) in the absence of exchange mixing of the levels with the aid of equation (5), or equivalently the matrix elements given in the upper part of table 2.

### 3.2. *Analysis of results with $S' = \frac{1}{2}$ model*

In order to fit the measured magnon dispersion (I) to the theoretical relations of § 3.1 we must first compensate for the effects of the magnon–phonon interaction as described in I.

To find the effective spin interaction parameters the data were fitted to the expression

**Table 3. Interaction parameters of $S' = \frac{1}{2}$ model**

| Number of parameters | Units | $H'_a$ | $J'_1$ | $J'_2$ | $J'_3$ |
|---|---|---|---|---|---|
| 3 | $cm^{-1}$ | 2·3 ± 0·7 | 39 ± 2 | 0·7 ± 0·5 | — |
| | THz | 0·07 ± 0·02 | 1·17 ± 0·06 | 0·02 ± 0·02 | — |
| 4 | $cm^{-1}$ | 3·1 ± 0·3 | 39 ± 1 | −0·1 ± 0·3 | −2·1 ± 0·2 |
| | THz | 0·09 ± 0·01 | 1·17 ± 0·02 | −0·00 ± 0·01 | −0·06 ± 0·01 |

The results of fitting the $S' = \frac{1}{2}$ model to the experimental results. $J'_r$ is the exchange constant between $r$th neighbour ions.

given in equation (11) by a least squares program (Powell 1965). The final values of the parameters are given in table 3, and in figure 2 the models are compared with experiment. The values of the small exchange constants $J'_2$ and $J'_3$ depend on whether $J'_3$ is fitted or not. Including $J'_3$ improves the fit although some of the $\langle\zeta\zeta\zeta\rangle$ points still lie off the calculated curve. In each fit $J'_1$ has essentially the same value, but $H'_a$ changes by about 30%. Since the effects of excited states have not been included, the dependence of these parameters

on the choice of model may be a result of the restriction to a $S' = \frac{1}{2}$ model. The errors quoted in table 3 are calculated from the variance–covariance matrix; the errors are, however, more dependent on the model chosen as can be seen by comparing the two fits.

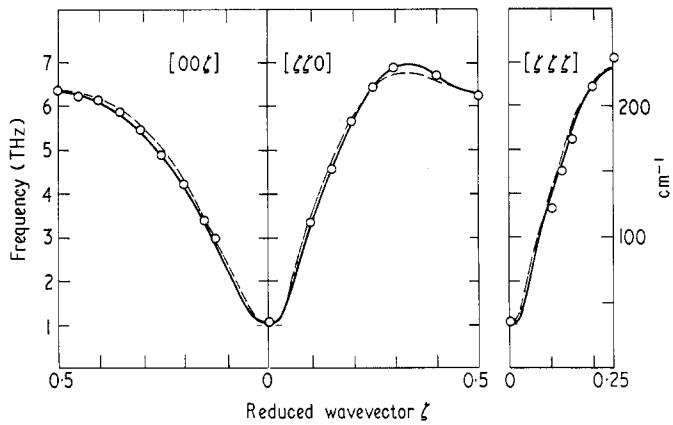


Figure 2. Result of fitting the spin $\frac{1}{2}$ model to the excitation of lowest energy in $KCoF_3$. Broken (solid) lines correspond to the three (four) parameter models given in table 3.

If the anisotropy energy arises from nearest neighbour anisotropic exchange, equation (6) we must interpret $J_1'$ as $J_1^{x'} = 39\,\mathrm{cm}^{-1}$ (1·17 THz) and $\Delta J_1' = J_1^{z'} - J_1^{x'} \simeq 0{\cdot}45\,\mathrm{cm}^{-1}$ (0·0135 THz).

Table 3 shows that for both fits the nearest neighbour exchange interaction is by far the largest as is usual in the perovskite structure (Windsor and Stevenson 1966, Pickart *et al.* 1966). The value found for $J_1'$ is consistent with the less accurate estimates from the Néel point and susceptibility measurements, as seen in table 4.

**Table 4. Comparison of values for the nearest neighbour exchange constant of $KCoF_3$ obtained by different methods**

| Obtained from | $J_1'$ ($\mathrm{cm}^{-1}$) | $J_2'$ ($\mathrm{cm}^{-1}$) |
|---|---|---|
| Neutron results | 39 ± 2 | 0·7 ± 0·5 |
| Néel temperature[a] | 40 | |
| Susceptibility of pairs[b] | 35 ± 5 | |

a, Using BPW relation (Smart 1959).
b, Sakamoto and Yamaguchi 1967.

The effective exchange constant $J_1'$ and anisotropy $H_a'$ may be related to the exchange and anisotropy interactions between real spins. To do this within the lowest pair of states by the molecular field approximation (see § 2.3) we describe the matrix elements of the real spin within this manifold in terms of the matrix elements of a fictitious spin $S' = \frac{1}{2}$. For an up-spin site.

$$S_z \rightarrow \tfrac{1}{2}c + bS_z'$$

$$S_+ \rightarrow KS_+'$$

where

$$c = \langle 0|S_z|0\rangle + \langle 1|S_z|1\rangle$$
$$b = \langle 0|S_z|0\rangle - \langle 1|S_z|1\rangle$$
$$K = \langle 0|S_+|1\rangle.$$

When the Hamiltonian is projected on to the lowest pair of states by means of this transformation we find the following relations

$$J = \frac{J'}{K^2}$$

$$H_a = \frac{H'_a}{b} - \frac{\Delta - 6J'}{b}$$

where $\Delta$ is the splitting of the ground state. For the case of no mixing the results are

$$J_1 = 0{\cdot}36\, J'_1 = 14\ \mathrm{cm}^{-1} = 0{\cdot}42\ \mathrm{THz}$$
$$H_a = 0{\cdot}6\, H'_a = 1{\cdot}6\ \mathrm{cm}^{-1} = 0{\cdot}05\ \mathrm{THz}.$$

When mixing is included the results are

$$J_1 = 0{\cdot}34\ J'_1 = 13{\cdot}3\ \mathrm{cm}^{-1} = 0{\cdot}40\ \mathrm{THz}$$
$$H_a = 0{\cdot}70\ H'_a = 2{\cdot}1\ \mathrm{cm}^{-1} = 0{\cdot}06\ \mathrm{THz}.$$

Note that for the particular set of parameters obtained in table 3, the exchange energy $6J'$ almost exactly cancels the molecular field energy $\Delta$ for the mixed states. $H_a$ is then independent of $J'$ but carries a large error because the exactness of the cancellation depends on the way in which the least squares fitting of the $S' = \frac{1}{2}$ model was performed. For the unmixed states the cancellation is, of course, exact. We conclude that the anisotropy of the system of real spins is small as we would expect from the fact that the lattice distortion below the Néel temperature is small. A comment on the value of the exchange $J_1$ obtained by this method will be made after analysis of the many level model.

3.3. *Lowest magnon mode with directional anisotropy*

Elliott and Thorpe (1968) have suggested that even in purely cubic fields it is possible for the interaction within the ground states to be of the form of equation (3) with anisotropy along the bond joining the ions. In the case of only nearest neighbour coupling the dispersion relation becomes

$$E(\boldsymbol{q}) = (\{H'_a + S'(4J'_{\|} + 8J'_{\perp}) \pm \{4S'J'_{\perp}(\cos q_z a + \cos q_y a) + 4S'J'_{\|}\cos q_x a\}\}$$
$$\times \{H'_a + S'(4J'_{\|} + 8J'_{\perp}) \mp \{4S'J'_{\perp}(\cos q_z a + \cos q_x a) + 4S'J'_{\|}\cos q_y a\}\})^{\frac{1}{2}}. \qquad (14)$$

This shows that the anisotropy removes the degeneracy between the two branches of the dispersion relation giving two modes. For small anisotropies the zone boundary energies $E(\frac{1}{2},0,0)$ and $E(0,\frac{1}{2},0)$ are $8\sqrt{2}S'J'_{\perp}$ and $8S'\{J'_{\|}(J'_{\perp} + J'_{\|})\}^{\frac{1}{2}}$ whereas $E(0,0,\frac{1}{2}) = 8S'\{J'_{\perp}(J'_{\perp} + J'_{\|})\}^{\frac{1}{2}}$. The splitting of the former modes, $\Delta E$, is therefore for small anisotropy in the exchange

$$\frac{\Delta E}{E} = \frac{3(J'_{\|} - J'_{\perp})}{4J'_{\perp}}.$$

Since the experimental measurements (I) did not show a detectable splitting it is concluded that $J'_{\|} - J'_{\perp}$ is less than 8% of $J'_{\perp}$. Recently Thorpe (private communication) has shown that in the strong field limit the dominant interelectron exchange integral in the kinetic exchange interaction gives a purely isotropic exchange interaction between real spins. A detailed analysis of this point must, however, await further theoretical developments.

## 4. The many level spin wave model

4.1. *Theory*

In this section the solution of the Hamiltonian equation (1) is described when excitations from the ground state to the eleven higher states of the $^4T_1$ level are included. The resultant branches of the dispersion relations are obtained by diagonalizing the quadratic Hamiltonian derived from an extension of the pseudoboson technique of Grover (1965). A similar calculation in which only the first two excited states were considered has been carried out for CoO (Sakurai *et al.* 1968). The method takes account of mixing between the different levels over and above that contained in the molecular field calculation of § 2.3.

The spin wave calculation starts from the energies $h\nu_p$ and states $|p\rangle$ of the single ion Hamiltonian, equation (10), in the molecular field approximation. In the pseudoboson approximation operators $a_p^+$ are introduced which excite an ion from the ground state 0 to the $p$th excited state. The spin operator of the $(jk)$ ion is then

$$\begin{aligned} S_+(jk) &\to \sum_p S_{+0}^{p}(k)\, a_p^+(jk) + S_{+p}^{0}(k) a_p(jk) \\ S_z(jk) &\to S_{z0}^{0}(k) + \sum_p S_{z0}^{p}(k)\{a_p^+(jk) + a_p(jk)\} \\ &\quad + \sum_p \{S_{zp}^{p}(k) - S_{z0}^{0}(k)\} a_p^+(jk) a_p(jk) \end{aligned} \tag{15}$$

where the matrix elements for $\alpha = +, -$ or $z$

$$S_{\alpha p'}^{p} = \langle p|S_\alpha|p'\rangle$$

are taken from the molecular field calculation (lower part of table 2). For the down spin sites ($k = 2$) the matrix elements may be seen from equation (10) to be related to those for $k = 1$ by changing $S_z \to -S_z$, $S_+ \to S_-$ and similarly for $l$. The single ion Hamiltonian is now diagonal:

$$\mathscr{H}^{(1)} = \sum_{jk} \sum_p h\nu_p a_p^+(jk)\, a_p(jk) \tag{16}$$

while the two-body remainder $\mathscr{H}^{(2)}$ provides the interactions between these localized excitations. The part of the total Hamiltonian $\mathscr{H}^{(1)} + \mathscr{H}^{(2)}$ which is quadratic in the Bose operators is then

$$\begin{aligned} \mathscr{H} = \tfrac{1}{2} \sum_{\boldsymbol{q}} \{ &\tilde{\boldsymbol{a}}^+(\boldsymbol{q})\, \mathbf{A}(\boldsymbol{q})\, \boldsymbol{a}(\boldsymbol{q}) + \tilde{\boldsymbol{a}}^+(-\boldsymbol{q})\, \mathbf{A}(-\boldsymbol{q})\, \boldsymbol{a}(-\boldsymbol{q}) \\ &+ \boldsymbol{a}^+(\boldsymbol{q})\, \mathbf{B}(q)\, \boldsymbol{a}^+(-\boldsymbol{q}) + \boldsymbol{a}(-q)\, \mathbf{B}(q)\, \boldsymbol{a}(q)\}. \end{aligned} \tag{17}$$

The column matrix $\boldsymbol{a}(\boldsymbol{q})$ has elements

$$a(kp, \boldsymbol{q}) = N^{-1/2} \sum_j a_p(jk) \exp\{i\boldsymbol{q} \cdot \boldsymbol{R}(jk)\} \tag{17a}$$

and the tensors are

$$\begin{aligned} \mathbf{A} &= \Delta + 2\mathbf{h}_{zz} + \mathbf{h}_{+-} + \mathbf{h}_{-+} \\ \mathbf{B} &= 2\mathbf{h}_{zz} + \mathbf{h}_{++} + \mathbf{h}_{--} \end{aligned} \tag{18}$$

where

$$h_{\alpha\beta}\begin{pmatrix} kk' \\ pp' \end{pmatrix} \boldsymbol{q} = J^{\alpha\beta}(kk'\boldsymbol{q})\, S_{\alpha 0}^{p}(k)\, S_{\beta p'}^{0}(k')$$

and $\Delta$ is the diagonal single ion matrix with elements $h\nu_p \delta_{pp'} \delta_{kk'}$.

The subscripts $\alpha, \beta = z, +$ or $-$ are introduced to describe anisotropy in the exchange if it is of the uniaxial form $J^{zz} \neq J^{+-}$.

The transformation to independent operators $\alpha(qs)$ (Walker 1963)

$$\begin{bmatrix} a(q) \\ a^*(-q) \end{bmatrix} = \begin{bmatrix} \mathbf{U}(q) & \mathbf{V}^*(-q) \\ \mathbf{V}(q) & \mathbf{U}^*(-q) \end{bmatrix} \begin{bmatrix} \alpha\ (q) \\ \alpha^*(-q) \end{bmatrix} \tag{19}$$

then leads to the usual energy matrix

$$\begin{pmatrix} \mathbf{A} & \mathbf{B} \\ -\mathbf{B} & -\mathbf{A} \end{pmatrix} \tag{20}$$

whose eigenvalues $\lambda$ in the case of centrosymmetric $KCoF_3$ may be shown to be given by the determinantal equation

$$|\mathbf{A}.\mathbf{A} - \mathbf{B}.\mathbf{B} + [\mathbf{A}, \mathbf{B}] - \lambda^2\mathbf{1}| \times |\mathbf{A}.\mathbf{A} - \mathbf{B}.\mathbf{B} - [\mathbf{A}, \mathbf{B}] - \lambda^2\mathbf{1}| = 0. \tag{21}$$

Only one determinant of this equation need be solved since the eigenvalues are simultaneous solutions of both determinants. We have therefore used equation (21) to obtain eigenvalues quickly as in the least squares fitting described in § 4.2. Although the commutator of **A** with **B** is zero for systems with only one excitation at each site, for example pure spin systems, it is nonzero for the case of $KCoF_3$ and has a marked effect on the frequencies of the excitations. Where eigenvectors were also required, as in the calculation of magnon intensities described in § 5, the original energy matrix, equation (20), was reduced to the solution of two 22 × 22 symmetric matrices by using the fact that **A** and **B** are separately symmetric. The eigenvectors of the problem are given in terms of the eigenvectors of both 22 × 22 matrices and are obtained more rapidly than by solution of the original 44 × 44 matrix.

Solutions for the 22 excitations for all wavevectors may now be obtained from equation (20). The excitations may be classified (see figure 4) into those involving only the $S^+$ and $S^-$ operators ($h_{zz} = 0$) which give doubly degenerate dispersion curves over the whole zone, and into those involving the $S_z$ operators ($h_{+-} = h_{-+} = 0$) which give rise in general to two distinct branches of the dispersion relations.

4.2. *Analysis of the results*

The theoretical model of the previous section was fitted to the results for the two branches of magnetic excitations of lowest frequency described in I. In the region of the magnon–

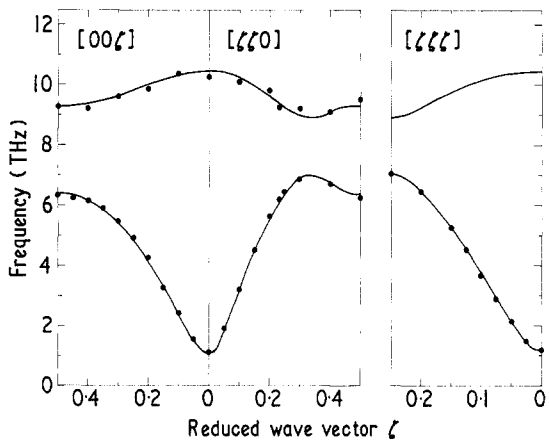


Figure 3. Dispersion curves of the lowest two excitations in $KCoF_3$ as measured by neutron inelastic scattering (circles) compared with the best many level model (B) with Heisenberg nearest neighbour exchange (curves).

**Table 5. Parameters obtained by fitting the many level model of the $^4T_1$ state to the experimental results**

| | $\chi$ | Units | $\Lambda$ | $c$ | $H_a$ | $J_1$ | $J_2$ |
|---|---|---|---|---|---|---|---|
| Model A | 0·84 | THz | 6·32 ± 0·06 | 0 | 0·06 ± 0·01 | 0·308 ± 0·005 | 0 ± 0·002 |
| | | $cm^{-1}$ | 211 ± 2 | 0 | 1·9 ± 0·5 | 10·3 ± 0·2 | 0 ± 0·1 |
| Model B | 0·82 | THz | 6·24 ± 0·06 | −0·26 ± 0·06 | 0 | 0·311 ± 0·001 | 0 |
| | | $cm^{-1}$ | 208 ± 2 | −9 ± 2 | 0 | 10·38 ± 0·04 | 0 |
| Model C | 1·55 | THz | 6·80 | 0 | 0·05 ± 0·03 | 0·309 ± 0·002 | 0 |
| | | $cm^{-1}$ | 227 | 0 | 1·8 ± 0·8 | 10·29 ± 0·07 | 0 |

phonon interaction the model was fitted to an interpolated 'pure magnon' dispersion curve, as described in § 3.2 of I, but the interpolated frequencies were given large errors.

The fits were performed with the Hamiltonian, equation (17), as obtained from equation (1) with parameters $c$, $\lambda$, $H_a$, and the nearest and next nearest neighbour exchange parameters $J_1$ and $J_2$, by using a least squares routine developed at Chalk River Nuclear Laboratories. The goodness of fit $\chi$ is the average ratio of the difference between experiment and model to the experimental error. All twelve levels of the $^4T_1$ state were included. The results of the fitting are summarized in table 5 and shown in figure 3, and supersede our earlier results (Buyers *et al.* 1968), which contained a numerical error.

Model A, in which the tetragonal distortion parameter $c$ was set to zero, gives an excellent description, $\chi = 0{\cdot}84$, of the experimental results. The anisotropy energy $H_a$ is small: if it is assumed to arise from anisotropic nearest neighbour exchange interactions the anisotropy is less than 2%, and is consistent with the results of the $S' = \frac{1}{2}$ model (see § 3.2). The next nearest neighbour exchange interaction is also small, as found for the $S' = \frac{1}{2}$ models, and was therefore set to zero in the other models discussed below.

The anisotropy parameter $H_a$ was set to zero in model B and an equally good fit, which is shown in figure 3, was obtained with a small value of the crystal field distortion parameter $c = -9 \pm 2$ cm$^{-1}$ ($-0{\cdot}27 \pm 0{\cdot}06$ THz). The small value of the distortion parameter is consistent with the value of the tetragonal distortion, $\delta a/a = 0{\cdot}0020$, measured by Okazaki and Suemune (1961). A direct calculation of $c$ using the point charge model of crystal field theory (for example see Hutchings 1964) assuming only the nearest neighbour fluorine atoms contribute gives

$$c = -\frac{6}{35}\frac{|Z_F|\,e^2}{R^3}\frac{\delta a}{a}\overline{r^2}(\alpha k_{orb})^2$$
$$= -8{\cdot}2\,|Z_F|\,\overline{r^2}\ \text{cm}^{-1}.$$

Here $-|Z_F|\,e$ is the apparent charge of a fluorine ion and $\overline{r^2}$ is the mean radius of the 3d electrons expressed in Å$^2$ in the second line. Thus the measured value of $c$ is of the order of that calculated on this model. Another method of estimating $c$ involves a comparison with $CoF_2$, whose crystal field parameters were deduced by Gladney (1966) from electron spin resonance data. If it is assumed that $\overline{r^2}$ is the same for $Co^{2+}$ in $KCoF_3$ as it is in $CoF_2$, $c$ may be obtained by scaling Gladney's tetragonal crystal field parameter by the ratio of the known tetragonal lattice distortions in $KCoF_3$ and $CoF_2$. This method gave $c \simeq -12$ cm$^{-1}$ which is again consistent with our experimental value.

In both models A and B the spin–orbit parameter is lower than would be expected for a free ion. In a crystalline environment the orbital angular momentum and spin–orbit parameter of the $Co^{2+}$ ion is reduced. Unfortunately no reliable measurements of the spin–orbit parameter in $KCoF_3$ exist. Thornley *et al.* (1965) deduced an effective spin–orbit parameter of $\lambda' = -160 \pm 10$ cm$^{-1}$ for the $^4T_1$ state from the susceptibility data of Hirakawa *et al.* (1960) and also obtained an orbital reduction factor $k_{orb} = 0{\cdot}93 \pm 0{\cdot}03$ from their measured $g$ value for the dilute salt. Ferguson *et al.* (1963), however, obtained $\lambda' = -167$ cm$^{-1}$ from optical absorption from the ground state to several excited states split by the spin–orbit coupling but several unexplained lines remained in their spectrum. If we assume both spin–orbit reduction and orbital reduction are separately effective then Thornley's results lead to $\Lambda = 212$ cm$^{-1}$ in good agreement with the directly observed value (model B) of 208 cm$^{-1}$, but if only spin–orbit reduction is important (ie it includes the effect of orbital reduction) we find the higher value $\Lambda = 227$ cm$^{-1}$. In model C the spin–orbit parameter was held fixed at this higher value while other parameters varied. Although a good fit with essentially unchanged exchange was found for the lower frequency branch, the overall fit as expected was worse ($\chi = 1{\cdot}55$) because the upper branch, whose energy is primarily determined by $\Lambda$, is about 7% too high. It is reasonable to assume that the upper frequency branch is only weakly dependent on the Heisenberg part of the exchange, for the energy of the zone boundary mode in the [111] direction contains less than 2% of

exchange energy, but this is not the case if more complex level dependent exchange caused by the orbital angular momentum is present. Copland and Levy (1970) estimate that the complex exchange may reduce the centre of the $j = \frac{3}{2}$ multiplet with respect to that of the $j = \frac{1}{2}$ multiplet by approximately 5%. This will lower the apparent spin–orbit parameter below the value appropriate to the high temperature susceptibility ($-160\ \mathrm{cm}^{-1}$) to a value of

$$\Lambda = 0{\cdot}95\alpha\lambda' = 216\ \mathrm{cm}^{-1}$$

in fair agreement with observation. In view of uncertainties in previous estimates of the spin–orbit parameter, we conclude that $\Lambda = 208\ \mathrm{cm}^{-1}$ from neutron scattering is likely

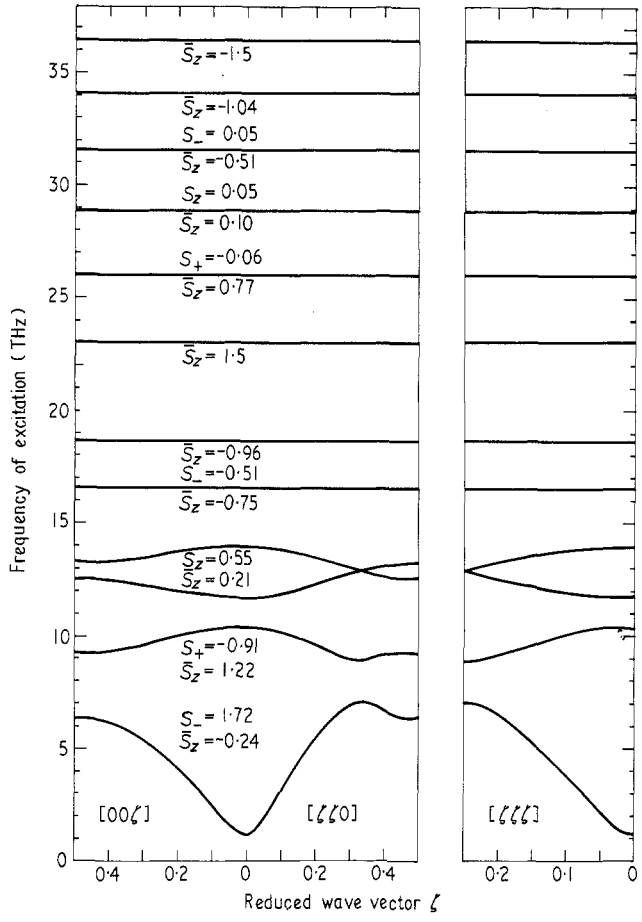


Figure 4. The dispersion curves of all distinct excitations associated with the $^4T_1$ orbital state in $KCoF_3$. The lowest two excitations are identical with those in figure 3. For each excitation we given the particular matrix element $\langle p|S_x|0\rangle$ associated with the transition if it is nonzero, and also the average value of spin $\bar{S}_z \equiv \langle p|S_z|p\rangle$.

the value of the apparent spin–orbit parameter that is best for calculating the ground state splitting. We may also conclude, since $\alpha = 1{\cdot}421$ is a well established number for the relation between $\boldsymbol{L}$ and $\boldsymbol{l}$, that the effective interaction between real angular momenta is $-\Lambda/\alpha = -146 \pm 2\ \mathrm{cm}^{-1}$ or 0·82 of the free ion value. It is not clear whether the reduction

arises in the real interaction in the orbital moment or from complex exchange, but our results do suggest that more than one process is important.

The exchange constants shown in table 5 are of the same order as those deduced from the values in table 3 for the $S' = \frac{1}{2}$ model, but are significantly lower by approximately 30%. They would therefore give very poor agreement with experiment if used, after projection, in the $S' = \frac{1}{2}$ model. The reason for this is sufficiently interesting to merit some discussion. One first notes that the $S' = \frac{1}{2}$ model is a two level model and, while one may obtain the correct mixing at the (111) zone boundary by projecting on to the molecular field states, one cannot take account of the variation of this mixing throughout the zone. For example, there is 20% of the molecular field state $p = 2$ mixed into the lowest frequency zone centre mode. Thus the parameters of table 5 used after projection in the $S' = \frac{1}{2}$ model (the theory of § 3.2 yields $J' = 31\ \mathrm{cm}^{-1}$, $H'_a = 48\ \mathrm{cm}^{-1}$) give the observed zone boundary frequency $234\ \mathrm{cm}^{-1}$ correctly but not the zone centre frequency $142\ \mathrm{cm}^{-1}$, which is much higher than the observed value of $36\ \mathrm{cm}^{-1}$. As a check on this behaviour, we have computed the $q = 0$ mode frequency when only one level is included in the calculation of the spin wave spectrum and the mixed molecular field states appropriate to the exchange in $KCoF_3$ are used. We find a frequency of $146\ \mathrm{cm}^{-1}$ in agreement with the results of the projected interaction. It seems therefore that the higher frequency excited states in the many level calculation reduce the zone centre frequency to the observed value of $36\ \mathrm{cm}^{-1}$. We conclude that the discrepancy between the exchange deduced from the $S' = \frac{1}{2}$ model and the many level model exists because the variation of the mixing of upper levels with wavevector is not included in the $S' = \frac{1}{2}$ model. In systems where the orbital momentum is unquenched, one must therefore be confident that the influence of states of higher energy is small before exchange constants between real spins may reliably be deduced from an $S' = \frac{1}{2}$ model, even when, as in the present case, this model gives a good description of the shape of the magnon branch of lowest energy.

The dispersion curves for all excitations of the $^4T_1$ orbital state predicted by our best model (B) are shown in figure 4. The results show that several higher excitations, which exist with an appreciable magnetic dipole moment strength, should be accessible to experimental study with high energy neutron sources or optical techniques.

## 5. The one magnon neutron cross section

In this section the intensity of neutrons scattered inelastically by a single magnon in a crystal of $KCoF_3$ is calculated and compared with experiment. The scattering length of a magnetic ion is taken in the small-$\boldsymbol{Q}$ approximation (Schwinger 1957) as proportional to the magnetic moment

$$\boldsymbol{M}(jk) = \boldsymbol{L}(jk) + 2\boldsymbol{S}(jk).$$

The true angular momentum is assumed to be related to the effective angular momentum by

$$\boldsymbol{L} = -\alpha k_{\mathrm{orb}} \boldsymbol{l}.$$

where $\alpha$ and $k_{\mathrm{orb}}$ are as given in § 2.1.

In the usual notation the differential cross section per cell for magnetic scattering from a crystal with atomic form factors $f_k(\boldsymbol{Q})$ is

$$S(\boldsymbol{Q},\omega) = \frac{1}{N}\left(\frac{\gamma e^2}{2mc^2}\right)^2 \sum_{jk}\sum_{j'k'} f_k(\boldsymbol{Q}) f_{k'}(\boldsymbol{Q}) \exp\left[\mathrm{i}\boldsymbol{Q}\cdot\{\boldsymbol{R}(jk) - \boldsymbol{R}(j'k')\}\right]$$
$$\times \sum_{\alpha\beta} \frac{1}{2\pi} \int \langle M_\alpha(jkt)\, M_\beta(j'k'0)\rangle \exp(\mathrm{i}\omega t)\, \mathrm{d}t\, (1 - Q_\alpha Q_\beta/Q^2) \qquad (22)$$

where $\langle\ \rangle$ denotes the thermal average. Equation (22) may be written in terms of a structure factor by transforming the components of $\boldsymbol{L}$ and $\boldsymbol{S}$ to Bose operators (see equation 15) and then transforming to magnon variables by equation (19). To do this we define row vectors on the up site ($k = 1$) by

$$(\boldsymbol{m}_+)_p = M_+{}^p_0(1)$$

and

$$(\boldsymbol{m}_z)_p = M_z{}^p_0(1)$$

and also divide the eigenvectors into parts associated with the up ($k = 1$) and down ($k = 2$) lattice of spins,

$$\begin{bmatrix} \boldsymbol{U} \\ \\ \boldsymbol{V} \end{bmatrix} \equiv \begin{bmatrix} \boldsymbol{U}_1 \\ \boldsymbol{U}_2 \\ \boldsymbol{V}_1 \\ \boldsymbol{V}_2 \end{bmatrix}.$$

The one magnon intensity in a multidomain specimen of $KCoF_3$ may then be written in terms of Bose occupation number $n_{qs}$ as

$$S(\boldsymbol{Q},\omega) = \left(\frac{\gamma e^2}{2mc^2}\right)^2 f^2(\boldsymbol{Q}) \sum_s |F(\boldsymbol{q}s)|^2 \{\delta(\omega + \omega_{\boldsymbol{q}s})\, n_{\boldsymbol{q}s} + \delta(\omega - \omega_{\boldsymbol{q}s})\,(n_{\boldsymbol{q}s} + 1)\} \times \sum_{\tau} \Delta(\boldsymbol{Q} + \boldsymbol{q} - \boldsymbol{\tau}) \tag{23}$$

with

$$|F(\boldsymbol{q}s)|^2 = \tfrac{2}{3}\,|\boldsymbol{m}_z \cdot (\boldsymbol{U}_1 - \boldsymbol{U}_2 + \boldsymbol{V}_1 - \boldsymbol{V}_2)|^2$$

for the $S_z$ modes, and

$$|F(\boldsymbol{q}s)|^2 = \tfrac{1}{3}\,|\boldsymbol{m}_+ \cdot (\boldsymbol{U}_1 \pm \boldsymbol{V}_2) + \boldsymbol{m}_- \cdot (\boldsymbol{V}_1 \pm \boldsymbol{U}_2)|^2 + \tfrac{1}{3}\,|\boldsymbol{m}_+ \cdot (\boldsymbol{V}_1 \pm \boldsymbol{U}_2) + \boldsymbol{m}_- \cdot (\boldsymbol{U}_1 \pm \boldsymbol{V}_2)|^2$$

for the $S_+$, $S_-$ modes. The upper signs apply in nuclear zones and the lower ones in magnetic zones.

The one magnon intensities in $KCoF_3$ have been computed from equation (23) with the eigenvectors and frequencies of the best model, B, and the form factor of Watson and Freeman (1961). The results are shown by the full curves in figure 5 for the two magnon branches of

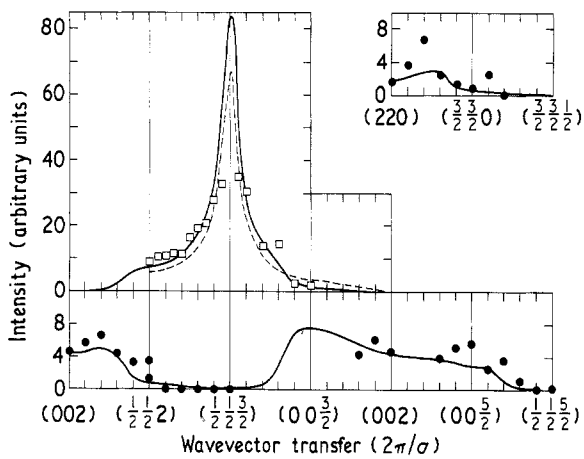


Figure 5. The intensity of one magnon scattering in $KCoF_3$ at low temperatures. The full curves are the predictions of the many level theory (model B) and the broken curve the $S' = \frac{1}{2}$ model. The integrated intensities of the peaks observed in neutron inelastic scattering experiments (see I) are shown as open squares for the branch of lowest frequency and full circles for the branch of higher frequency. The wave vector transfer $\boldsymbol{Q}$ is plotted uniformly along straight lines in reciprocal space joining the wave vectors given as abscissae in units $2\pi/a$.

lowest frequency. The intensity given by the $S' = \frac{1}{2}$ model was obtained by projecting the magnetic moment on to the lowest two states as

$$M_+ = M_+ {}^0_1 S'_+ = 4{\cdot}26 S'_+$$

and then using the results of § 3.2. The intensity on this model is shown by the broken curve and differs slightly from the result of the many level theory for the lowest energy magnon. The $S' = \frac{1}{2}$ theory cannot, of course, describe the magnon of higher energy.

The measured intensities of several magnons described in I are also shown on figure 5. These are integrated intensities of observed neutron groups and have been put on a relative scale by making allowance for changes in instrumental resolution where necessary, and they have also been normalized overall to the intensity given by the many level theory at $\boldsymbol{Q} = 2\pi a^{-1}$ (0·5, 0·5, 0·8). The measurements are probably good to 30% at best as no corrections have been made for such effects as specimen absorption, multiple scattering. Bearing this in mind, the theory is seen from figure 5 to be in satisfactory agreement with experiment over a wide range of wavevectors. In particular, the theory correctly predicts for the magnon of higher energy the strong scattering found in the nuclear zone, and the near absence of magnetic scattering near the centre of magnetic zones. This cancellation may be seen from the eigenvectors of the magnons to be related to the opposite signs (table 2) for the matrix elements $\langle 1 | S_- | 0 \rangle$ and $\langle 2 | S_+ | 0 \rangle$ connecting the ground state with the first two excited states. These results in addition to providing an approximate check on the eigenvectors of the many level model, also serve to confirm that the mode of higher energy is magnetic.

## 6. The magnon–phonon interaction

One of the features of the experimental results described in I was the observation of a strong interaction which prevented the crossing of the magnon and phonon branches near $\boldsymbol{q} = 0$. This is not surprising for, although no forbidden crossings were observed for the magnons in the related crystal $CoF_2$ (Martel *et al.* 1968), Allen and Guggenheim (1968) found that significant coupling to the $E_u$ phonons was present. The origin of this interaction is discussed in the present section. A strong magnon–phonon interaction has been observed before in $UO_2$ (Dolling and Cowley 1966) and in that case was shown to arise from the fluctuations in the crystal field due to the motions of the atoms (Cowley and Dolling 1968). In this section we discuss possible mechanisms for the magnon–phonon interaction and find that the crystal field mechanism proposed for $UO_2$ plays a part even for an odd electron ion such as $Co^{2+}$.

### 6.1. *Crystal field effects*

The magnon–phonon interaction was observed to be strong in the neighbourhood of the magnetic reciprocal lattice point. At that point in reciprocal space the phonon was shown in I to have the symmetry $\Gamma_{25}$ with the convention that the potassium atom is at the origin of the unit cell. The orbital momentum operators $l = 1$ in the $^4T_1$ ground state also transform as $\Gamma_{25}$. Consequently, the phonon mode is able to cause transitions within the different orbital states of the $^4T_1$ triplet.

The magnon–phonon interaction arising from the crystal field is evaluated in the following way. We assume that the eigenvectors of the phonon and magnon vary sufficiently slowly that it is adequate to calculate the interaction at the magnetic zone centre. The basic interaction is that between the electrons on the $Co^{2+}$ ion and the fluctuating Coulomb potential of the surrounding ions. Within the point-ion model we consider only the effect of the motion of the nearest neighbour fluorine ions of charge $-|Z_F|e$, where $e$ is the absolute magnitude of the electronic charge. The lowest order term that will produce a magnon–phonon interaction will be linear in the phonon and magnon variables and may thus be found from the field of the dipoles $-|Z_F| e \boldsymbol{U}_F$ produced by the fluorine displacements

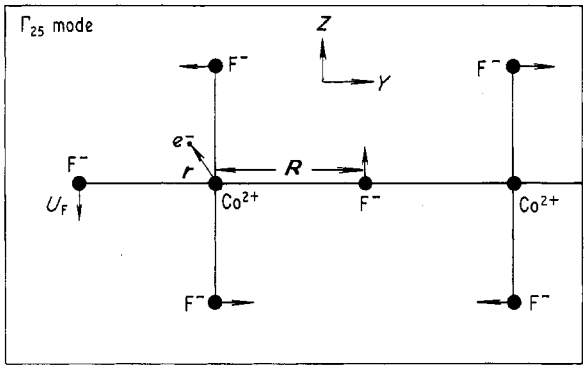


Figure 6. The pattern of atomic displacement in $KCoF_3$ in the phonon mode $\Gamma_{25}$ of wavevector $\boldsymbol{q} = (\frac{1}{2}, \frac{1}{2}, \frac{1}{2})2\pi/a$ and of lowest frequency. Only the $(y, z)$ component of this triply degenerate phonon is shown.

$\boldsymbol{U}_F$ occurring in the $\Gamma_{25}$ mode as shown in figure 6. The change in the energy of a single cobalt ion is then

$$V_{\text{ion}} = |Z_F| e^2 \sum_{\boldsymbol{r}} \sum_{\boldsymbol{R}} \frac{\boldsymbol{U}_F(\boldsymbol{R}) . (\boldsymbol{r} - \boldsymbol{R})}{|\boldsymbol{r} - \boldsymbol{R}|^3} \tag{24}$$

where the sums are over the magnetic electrons $\boldsymbol{r}$ and the nearest neighbour fluorine ions $\boldsymbol{R}$.

For the $\Gamma_{25}$ mode the lowest nonzero terms in the expansion in powers of the electron coordinates are those of fourth order which are of the form

$$V_{\text{ion}} = |Z_F| e^2 U_F \frac{2240}{a^6} \sum_{\boldsymbol{r}} (y^3 z - z^3 y) \tag{25}$$

for the mode polarized in the $(yz)$ plane where $a$ is the cobalt–cobalt distance. Similar expressions are obtained for the other two modes by permutation of $x, y, z$. Within a manifold of constant $l$ we may write

$$\sum_{\boldsymbol{r}} (y^3 z - z^3 y) = \frac{\beta}{4} \overline{r^4} (\alpha k_{\text{orb}})^4 \, O(y, z) \tag{26}$$

where

$$O(y, z) = l_y^3 l_z + l_y^2 l_z l_y + l_y l_z l_y^2 + l_z l_y^3 - l_z^3 l_y - l_z^2 l_y l_z - l_z l_y l_z^2 - l_y l_z^3. \tag{27}$$

The averaged fourth power of the radius of the magnetic electrons is $\overline{r^4}$ and $\beta = -2/315$.

When the operator $O$ is projected into the space spanned by the lowest two states of the $Co^{2+}$ ion, the terms which are linear in the Bose operators are

$$\begin{aligned} O(y, z) &= id(l) \{a^+(jk) - a(jk)\} \\ O(z, x) &= d(l) \{a^+(jk) + a(jk)\} (-1)^{k-1} \end{aligned} \tag{28}$$

where

$$d(l) = 0{\cdot}10 \tag{29}$$

for the mixed states of tables 1 and 2.

The form of the operator $O(x, y)$ shows that the $xy$ phonon mode cannot interact with the $\Gamma_{25}$ magnon in the present approximation, and only the other two members of the triply degenerate $\Gamma_{25}$ phonon are important.

Introducing the phonon operators $b(yz)$ and $b(zx)$ belonging to the two important

polarizations of the $\Gamma_{25}$ mode (frequency $\omega_p$) and the magnon operators $\alpha(1)$ and $\alpha(2)$ for the two degenerate magnons (frequency $\omega_m$) we finally obtain the interaction Hamiltonian

$$\frac{\mathscr{H}_{mp}}{\hbar} = \omega_m\alpha^+(1)\,\alpha(1) + \omega_m\alpha^+(2)\,\alpha(2) + \omega_p b^+(yz)\,b(yz) + \omega_p b^+(zx)\,b(zx)$$
$$+ K\{\alpha^+(1)\,b(yz) - \alpha(1)b^+(yz) + \alpha(2)b^+(yz) - \alpha^+(2)\,b(yz)$$
$$+ \alpha^+(1)\,b(zx) + \alpha(1)\,b^+(zx) + \alpha(2)b^+(zx) + \alpha^+(2)\,b(zx)\}$$

where

$$K = 0{\cdot}10\,|Z_F|\,e^2U_F560\beta\,\frac{\overline{r^4}}{a^6}(\alpha k_{orb})^4\,(f+g)$$
$$= 0{\cdot}013\,|Z_F|\ \text{THz}.$$

We have used the value $\overline{r^4} = 0{\cdot}5$ Å$^4$ estimated by Watson (1959) and calculated the magnon eigenvectors $f$ and $g$ from a spin $\frac{1}{2}$ model that fits the observed zone boundary frequency and a frequency at $\boldsymbol{q} = 0$ of 1·4 THz, assumed to be the same for magnon and phonon. The final strength of the magnon–phonon interaction determined as the half splitting at $q = 0$ is, for $|Z_F| = 1$,

$$\epsilon = \sqrt{2K} = 0{\cdot}02\ \text{THz}.$$

We note that the interaction is only possible because of exchange mixing of the lowest Kramer's doublet with higher states, and that the lowest nonzero term in the potential of the $\Gamma_{25}$ mode is fourth order in the electron coordinates. Nonetheless the calculation shows that the phonon modulated crystal field mechanism cannot be neglected when considering the magnon–phonon interaction. That the calculated result is low compared with experiment (0·35 THz) may possibly be a result of using the point ion model for the crystal field perturbation or of performing the calculation at $\boldsymbol{q} = 0$ instead of in the region of crossover at $|\boldsymbol{q}| = 0{\cdot}07\ 2\pi/a$. It is also possible that the crystal field effect might be enhanced if orbital effects were correctly taken into account.

6.2. *Exchange effects*

It is also possible for a magnon–phonon interaction to result from the modulation of the exchange interactions by the motions of the atoms. One of the most direct ways in which this can occur is through the dependence of the exchange constant in the Heisenberg Hamiltonian, equation (4), on the distance between the ions. The changes in this distance due to the presence of the phonons then modify the exchange giving rise to a magnon–phonon interaction.

This mechanism is not thought to be appropriate to $KCoF_3$. Firstly, in the $\Gamma_{25}$ normal mode the Co atoms do not move. Secondly, this process gives rise to terms in the Hamiltonian which contain two spin wave operators and a single phonon operator. These give rise to magnon–phonon interaction only in higher order perturbation theory than do the terms linear in the spin wave operators discussed in § 6.1.

Magnon–phonon interaction may also arise through the exchange if the displacements of the atoms give rise to anisotropic terms in the exchange energy. In the $\Gamma_{25}$ mode the fluorine atoms move perpendicular to the bond joining the two magnetic ions. This may give rise to an anisotropic exchange between the atoms, which for a bond direction in the $z$ direction is of the form

$$G(12)\,u_\alpha(F)\,\{S_\alpha(1)\,S_z(2) + S_\alpha(2)\,S_z(1)\}$$

where $u_\alpha(F)$ is the amplitude of motion of the intervening fluorine atom in the $\alpha = x$ or $y$ direction, and $G$ is the appropriate constant. This gives rise to a term in the Hamiltonian which is linear in both the phonon operators and the magnon operators and hence is a

possible origin of the interaction in $KCoF_3$. Unfortunately in view of the uncertainties in the details of the superexchange between $Co^{2+}$ ions it is at present impossible to even estimate the magnitude of this effect. However, we believe that this is not the cause of the magnon–phonon interaction in $KCoF_3$; firstly, because of the importance of the crystal field mechanism described in § 6.1 and secondly, because no evidence for anisotropic exchange was found in the spin wave measurements, § 3.3, it is probable that the effect of the phonon modulated exchange is small.

## 7. Summary

We have described the magnetic excitations of $KCoF_3$ at low temperatures. The results show that the lowest branch of the spin wave dispersion curves may be described by an effective spin $\frac{1}{2}$ model with an isotropic Heisenberg exchange constant and a small anisotropy. The value of the exchange constants are consistent with those deduced from the Néel temperature using the cluster model of Smart (1959) and from the susceptibility of pairs deduced by Sakamoto and Yamaguchi (1967), as listed in table 5.

A model involving excitations to all eleven states of the $^4T_1$ orbital triplet gives an excellent description of the dispersion curves obtained by neutron inelastic scattering (I) when the Heisenberg form of exchange interaction is assumed. The value of the spin–orbit constant is found to be somewhat less than that obtained by Thornley *et al.* (1965) from susceptibility measurements.

These results are somewhat surprising because the exchange interactions in $KCoF_3$ are expected to be anisotropic and to differ from one level to another. Our results suggest that at least for the lowest excitation the exchange is considerably simpler in form than has been suggested by the theoretical work of Elliott and Thorpe (1968) and Copland and Levy (1970). The reduction in the magnitude of the spin–orbit parameter possibly results from a different exchange interaction with the excited states of high frequency as suggested by Copland and Levy (1970).

The intensity of one magnon scattering has been computed from the many level model and good agreement found for both magnetic branches. This forms an approximate check on the eigenvectors of the model and provides further confirmation that the branch of higher energy is magnetic.

The magnon–phonon interaction in $KCoF_3$ has also been discussed. It is shown that the distortion of the crystal field by the phonon can give a significant contribution to the magnon–phonon interaction. We cannot, however, rule out the possibility that part of the interaction results from a modification of the exchange by the phonons.

In the experimental paper of this series (I) measurements of the temperature dependence of the magnons were presented. No attempt has as yet been made to calculate these in detail and this must await further developments.

## Acknowledgments

We have benefitted from useful discussions with many colleagues, in particular with the staff of the computation centre at Chalk River and with Paul Lee. The work was performed under the auspices of the U.S. Atomic Energy Commission.

## References

ABRAGAM, A., and PRYCE, M. H. L., 1951, *Proc. R. Soc.* A, **206**, 173–91.
ALLEN, S. J., and GUGGENHEIM, H. J., 1968, *Phys. Rev. Lett.*, **21**, 1807–10.
BIRGENEAU, R. J., HUTCHINGS, M. T., BAKER, J. M., and RILEY, J., 1969, *J. appl. Phys.*, **40**, 1070–9.
BUYERS, W. J. L., *et al.*, 1968, *Proc. 11th Int. Conf. Low Temp. Phys., St. Andrews* (St. Andrews: University of St. Andrews Press), pp. 1330–5.
COPLAND, G. M., and LEVY, P. M., 1970, *Phys. Rev.*, **B1**, 3043–50.
COWLEY, R. A., 1964, *Phys. Rev.*, **134**, A981–97.
COWLEY, R. A., and DOLLING, G., 1968, *Phys. Rev.*, **167**, 464–77.
DOLLING, G., and COWLEY, R. A., 1966, *Phys. Rev. Lett.*, **16**, 683–5.

ELLIOTT, R. J., and THORPE, M. F., 1968, *J. appl. Phys.*, **39**, 802–7.
FERGUSON, J., WOOD, D. L., and KNOX, K., 1963, *J. chem. Phys.*, **39**, 881–9.
GLADNEY, H. M., 1966, *Phys. Rev.*, **146**, 253.
GROVER, B., 1965, *Phys. Rev.*, **140**, A1944–51.
HIRAKAWA, K., HIRAKAWA, K., and HASHIMOTO, T., 1960, *J. Phys. Soc. Japan*, **15**, 2063–8.
HOLDEN, T. M., *et al.*, 1971, *J. Phys.* C: *Solid St. Phys.*, **4**, 2127–38.
HUTCHINGS, M. T., 1964, *Solid State Physics*, Vol. 16 (New York: Academic Press), pp. 227–73.
LEVY, P. M., 1964, *Phys. Rev.*, **135**, A155–65.
—— 1966, *Phys. Rev.*, **147**, 311–9.
MARTEL, P., COWLEY, R. A., and STEVENSON, R. W. H., 1968, *Can. J. Phys.*, **46**, 1355–70.
OKAZAKI, A., and SUEMUNE, Y., 1961, *J. Phys. Soc. Japan*, **16**, 671–5.
PICKART, S. J., COLLINS, M. F., and WINDSOR, C. G., 1966, *J. appl. Phys.*, **37**, 1054–5.
POWELL, M. J. D., 1965, *Computer J.*, **7**, 303–7.
SAKAMOTO, N., and YAMAGUCHI, Y., 1967, *J. Phys. Soc. Japan*, **22**, 885–91.
SAKURAI, J., BUYERS, W. J. L., COWLEY, R. A., and DOLLING, G., 1968, *Phys. Rev.*, **167**, 510–8.
SCHWINGER, J., 1937, *Phys. Rev.*, **51**, 544–52.
SMART, J. S., 1959, *J. Phys. Chem. Solids*, **11**, 97–104.
STEVENS, K. W. H., 1953, *Proc. R. Soc.* A, **219**, 542–55.
SVENSSON, E. C., *et al.*, 1969, *Can. J. Phys.*, **47**, 1983–8.
THORNLEY, J. H. M., WINDSOR, C. G., and OWEN, J., 1965, *Proc. R. Soc.* A, **284**, 252–71.
VAN VLECK, J. H., 1962, *Revista de Mathematica y Fisica Theorica*, **14**, 189–96.
WALKER, L. R., 1963, *Magnetism*, eds G. T. Rado and H. Suhl, Vol. 1 (New York: Academic Press), pp. 299–381.
WATSON, R. E., 1959, *M.I.T. Tech. Rep* No. 12.
WATSON, R. E., and FREEMAN, A. J., 1961, *Acta. Crystallogr.* **14**, 27–37.
WINDSOR, C. G., and STEVENSON, R. W. H., 1966, *Proc. Phys. Soc.*, **87**, 501–4.